AFRL-RW-EG-TP-2008-7421

NUMERICAL MODELING OF HETEROGENEOUS HIGH EXPLOSIVES (CONFERENCE PAPER AND BRIEFING CHARTS)

Christopher M. Engelhardt
Air Force Research Laboratory
Munitions Directorate
AFRL/RWAC
Eglin AFB, FL 32542-6810

SEPTEMBER 2008

CONFERENCE PAPER AND BRIEFING CHARTS

This paper and briefing charts were presented at the 40th AIAA Thermophysics Conference, June 23-26, 2008, in Seattle, Washington. The paper has been published by the American Institute of Aeronautics and Astronautics (AIAA) as AIAA 2008-3921.

DISTRIBUTION A: Approved for public release; distribution unlimited.
Paper approval confirmation 96 ABW/PA # 05-27-08-267; dated 27 May 2008.
Briefing Charts approval confirmation 96 ABW/PA # 06-13-08-296; dated 13 June 2008.

REPORT DOCUMENTATION PAGE

Form Approved
OMB No. 0704-0188

PLEASE DO NOT RETURN YOUR FORM TO THE ABOVE ADDRESS.

1. REPORT DATE *(DD-MM-YYYY)*	2. REPORT TYPE	3. DATES COVERED *(From - To)*
XX-09-2008	CONFERENCE PAPER AND BRIEFING CHARTS	

4. TITLE AND SUBTITLE

NUMERICAL MODELING OF HETEROGENEOUS HIGH EXPLOSIVES (CONFERENCE PAPER AND BRIEFING CHARTS)

5a. CONTRACT NUMBER

N/A

5b. GRANT NUMBER

N/A

5c. PROGRAM ELEMENT NUMBER

N/A

6. AUTHOR(S)

Christopher M. Engelhardt

5d. PROJECT NUMBER

N/A

5e. TASK NUMBER

N/A

5f. WORK UNIT NUMBER

N/A

7. PERFORMING ORGANIZATION NAME(S) AND ADDRESS(ES)

Air Force Research Laboratory
Munitions Directorate
AFRL/RWAC
Eglin AFB, FL 32542-6810

8. PERFORMING ORGANIZATION REPORT NUMBER

AFRL-RW-EG-TP-2008-7421

9. SPONSORING/MONITORING AGENCY NAME(S) AND ADDRESS(ES)

Air Force Research Laboratory
Munitions Directorate
AFRL/RWAC
Eglin AFB, FL 32542-6810

10. SPONSOR/MONITOR'S ACRONYM(S)

AFRL-RW-EG

11. SPONSOR/MONITOR'S REPORT NUMBER(S)

SAME AS BLOCK 8

12. DISTRIBUTION/AVAILABILITY STATEMENT

DISTRIBUTION A: Approved for public release; distribution unlimited.
Approval confirmation 96 ABW/PA # 05-27-08-267; dated 27 May 2008.
Approval confirmation 96 ABW/PA # 06-13-08-296; dated 13 June 2008.

13. SUPPLEMENTARY NOTES

See 'cover page' for pertinent metadata information.

14. ABSTRACT

This report contains a numerical algorithm for modeling the detonation and explosion of a heterogeneous mixture of high explosive and small metal particles. The simulation examines a spherical explosive design with a mixture of nitromethane as the high explosive and steel as the metal particles. The algorithm provides a computational model of the detonation and explosion by producing position, velocity, and temperature profiles for the metal particles over time. For the gas phase, the algorithm produces position, velocity, temperature, density, and pressure profiles over time. This is accomplished by taking into account the initial position and velocity profiles for the metal particles, a corresponding particle drag law, appropriate explosive energy and detonation pressure inputs, and a blast wave solution that governs the thermodynamic state of the gas phase. The behavior of the solid particles and gas phase throughout the explosion is simulated by a coupled, two-phase algorithm. The results of the model are compared against experimental data and critiqued on a theoretical level as well. Recommendations and plans for improvements to the algorithm are discussed. This model is intended to provide a sound representation of the detonation as well as insight into the behavior of a heterogeneous explosive.

15. SUBJECT TERMS

N/A

16. SECURITY CLASSIFICATION OF:			17. LIMITATION OF ABSTRACT	18. NUMBER OF PAGES	19a. NAME OF RESPONSIBLE PERSON
a. REPORT	b. ABSTRACT	c. THIS PAGE			Christopher M. Engelhardt
UNCLASSIFIED	UNCLASSIFIED	UNCLASSIFIED	SAR	32	19b. TELEPHONE NUMBER *(Include area code)*

Numerical Modeling of Heterogeneous High Explosives

Christopher M. Engelhardt[1]
Air Force Research Laboratory, Eglin AFB, FL 32542, USA

This report contains a numerical algorithm for modeling the detonation and explosion of a heterogeneous mixture of high explosive and small metal particles. The simulation examines a spherical explosive design with a mixture of nitromethane as the high explosive and steel as the metal particles. The algorithm provides a computational model of the detonation and explosion by producing position, velocity, and temperature profiles for the metal particles over time. For the gas phase, the algorithm produces position, velocity, temperature, density, and pressure profiles over time. This is accomplished by taking into account the initial position and velocity profiles for the metal particles, a corresponding particle drag law, appropriate explosive energy and detonation pressure inputs, and a blast wave solution that governs the thermodynamic state of the gas phase. The behavior of the solid particles and gas phase throughout the explosion is simulated by a coupled, two-phase algorithm. The results of the model are compared against experimental data and critiqued on a theoretical level as well. Recommendations and plans for improvements to the algorithm are discussed. This model is intended to provide a sound representation of the detonation as well as insight into the behavior of a heterogeneous explosive.

Nomenclature

V_d	=	detonation velocity	E_b	=	blast wave energy
E_g	=	Gurney energy	γ	=	ratio of specific heats
M_g, M_p	=	total mass of explosive and metal	a	=	speed of sound
R	=	radius	t	=	time
F_d	=	drag force on metal particle	η	=	function of radius
d	=	particle diameter	ϕ	=	velocity function
C_d	=	drag coefficient	f	=	pressure function
ρ	=	gas density	ψ	=	density function
v_g, v_p	=	gas and particle velocity	β	=	function of specific heat
μ	=	dynamic viscosity	P	=	pressure
α_g, α_p	=	gas and particle volume concentration	M	=	mach number
$\dot{q}$	=	heat transfer rate	δ	=	function of specific heat
λ	=	thermal conductivity coefficient	x	=	position
C_p	=	specific heat	a_i	=	initial speed of sound
m	=	particle mass	w	=	function of velocity and speed of sound
T	=	temperature	Q	=	function of velocity and speed of sound

I. Introduction

THERE have been several theoretical methods developed that model the detonation and explosion of a high explosive. The addition of many small metal particles into the high explosive to create a heterogeneous mixture has recently been studied. In 1986, Baer and Nunziato described a two-phase model using reactive granular materials. Their study used a continuum theory which considered compressibility, entropy inequality, and accounted for mass, momentum, and energy exchange.[1] In 1992, Lanovets conducted a numeric study on inert solid particles

[1] Physicist, Computational Mechanics Branch, Munitions Directorate.

contained in a spherical charge. This investigation considered a continuum of detonation gas combined with heavy particles.[2] Another study that was performed by Patankar and Joseph in 2001 describes particle flow using an Eulerian-Lagrangian setup for the fluid phase and the solid phase respectively. The simulation by Patankar and Joseph emphasized flexibility in forces being modeled, differing particle sizes and properties, dense flow, and conservative computing requirements.[3] Powers followed the previous work and examined granular energetic materials using a two-phase model in 2004.[4]

Using numerical techniques to model the two-phase flow of a heterogeneous high explosive requires a velocity initialization scheme to capture the initial detonation acceleration as well as a blast wave solution for subsequent acceleration. The Gurney Equations were derived in 1943 as a simple way to approximate the velocity of the explosive shell fragments. This was accomplished using an energy balance between the kinetic energy of the explosive gas and shell fragments with the chemical energy of the explosive.[5] Two different blast wave solutions have been proposed, one by Taylor in 1949 and another in 1961 by Friedman. These blast wave solutions serve to determine the flow properties after the initial detonation.[12,13] In 2007, Frost performed experiments which tracked the explosive clouds created by the detonation of a heterogeneous mixture of Nitromethane and steel particles.[6,7] The Frost study will provide a basis to compare the numeric simulation to experimental data. The purpose of this study is to construct and analyze a numeric algorithm based on theoretical methods which can accurately model the detonation and two-phase flow of a heterogeneous high explosive.

II. Technical Approach

A. Velocity Initialization

The inert metal particles experience an initial acceleration during the detonation of the high explosive followed by further acceleration due to the resulting blast wave flow. It is necessary to determine the velocity of the particles and gas from detonation which is used as an initial condition in the algorithm. One way to approximate this initialization is to modify the Gurney equations. The Gurney method has been used to estimate the velocity profile of explosive gasses and surrounding shell case. These equations are derived from an energy balance between the Gurney energy of the high explosive used and the kinetic energy of the gas phase and shell fragments.[5] The Gurney equations require modification in order to approximate a heterogeneous mixture. The original Gurney equations assume a continuous mass of high explosive surrounded by one solid shell. These equations can be modified to include several extremely small layers of explosive mass and metal particles which, when solved iteratively from the core to the outer explosive edge provide a velocity profile. Many repeated and very thin explosive layers will approximate a heterogeneous mixture. The result is shown below in Eq. (1) where R_o and R_i are the outer and inner radii of the layer in question. This provides the basis for the initial detonation velocity of the metal particles and the initial gas phase velocity profile.

$$V_d = \sqrt{2E_g}\left(\frac{M_p}{M_g}+\frac{3}{5}\left[1-\frac{3R_oR_i+5R_i^{\,2}}{6\left(R_o^{\,2}+R_oR_i+R_i^{\,2}\right)}\right]\right)^{\frac{-1}{2}} \tag{1}$$

B. Particle Drag and Heat Transfer

Several drag laws and heat transfer laws were tested during the construction of the model. The equations that were found to be the most accurate for this type of experiment were outlined by Akhatov and are described below.[8] Each spherical particle experiences a drag force given by Eq. (2). This force accounts for varying Reynolds numbers given by Eq. (3) and a piecewise defined drag coefficient that is dependent on both the Reynolds number and the particle volume concentration shown in Eq. (4). The heat transfer law shown in Eq. (5) accounts for varying Nusselt numbers, N_u, by Eq. (6) where Re is the Reynolds number and Pr is the Prandtl number. Reynolds numbers, Nusselt numbers, and drag coefficients are updated at each time step for each individual particle.

$$F_d = \frac{\pi d^2}{4} C_d \rho \frac{\left|v_g - v_p\right|\left(v_g - v_p\right)}{2} \tag{2}$$

$$\mathrm{Re} = \rho\left|v_g - v_p\right| d / \mu \tag{3}$$

$$C_d = \begin{cases} C_1 = \dfrac{24}{\mathrm{Re}} + \dfrac{4.4}{\mathrm{Re}^{0.5}} + 0.42 & \alpha_p \le 0.08 \\ C_2 = \dfrac{4}{3\alpha_g}\left(1.75 + \dfrac{150\alpha_p}{\alpha_g \,\mathrm{Re}}\right) & \alpha_p \ge 0.45 \\ C_3 = \dfrac{(\alpha_p - 0.08)C_2 + (0.45 - \alpha_p)C_1}{0.37} & 0.08 < \alpha_p < 0.45 \end{cases} \tag{4}$$

$$\dot{q} = \pi d \lambda N_u (T_g - T_p)/(mC_p) \tag{5}$$

$$N_u = \begin{cases} 2 + 0.106\,\mathrm{Re}\,\mathrm{Pr}^{0.33} \\ 2.274 + 0.6\,\mathrm{Re}^{0.67}\,\mathrm{Pr}^{0.33} \end{cases} \tag{6}$$

C. Taylor's Blast Wave Solution

Two different blast wave solutions were analyzed during the construction of this algorithm. The simpler solution was developed by Taylor. This similarity solution creates position, velocity, pressure, density, and temperature profiles over time quantified primarily by the blast wave energy of the specific explosion and derived from the continuity of mass, momentum, and energy laws. We apply Taylor's approximate form of this similarity solution. Defining the blast wave energy as the chemical energy released during detonation of the explosive allows solving for the parameter, *A*, in Eq. (7) which is used in subsequent calculations.[10] Taylor calculates the blast radius as a function of the constant, *A*, and time as in Eq. (8).[12] The zero subscript refers to the ambient condition.

$$E_b = A^2 \rho_0 \left(2\pi(0.185) + \frac{4\pi}{\gamma(\gamma - 1)}(0.187)\right) \tag{7}$$

$$R(t) = (2.5A)^{2/5} t^{2/5} \tag{8}$$

To determine the gas phase velocity profile, the function η is the dimensionless radius of the blast wave's interior equal to the local radius divided by the radius of the outer blast wave at any given time as shown in Eq. (9). Three other functions of η are ϕ, *f*, and ψ which represent the non-dimensional velocity, pressure, and density profiles respectively. Scaling these quantities requires multiplying by appropriate parameters as defined in Eqs. (10) through (15). For simplicity, β is defined in Eq. (16). With these profiles, temperature can also be calculated by using the assumption of a calorically perfect gas shown in Eq. (17).[9,10,11,12]

$$\eta = r / R(t) \tag{9}$$

$$v_g = AR^{-3/2}\phi(\eta) \tag{10}$$

$$\phi(\eta) = (\eta / \lambda) + \eta^{\beta} / \gamma \tag{11}$$

$$P = P_0 A^2 R^{-3} f(\eta) / a_0^{\,2} \tag{12}$$

$$f(\eta) = \exp\left\{\ln\left(\frac{2\gamma}{\gamma + 1}\right) - \left(\frac{2\gamma^2 + 7\gamma - 3}{7 - \gamma}\right)\ln\left(\frac{\gamma + 1 - \eta^{\beta - 1}}{\gamma}\right)\right\} \tag{13}$$

$$\rho = \rho_0 \psi(\eta) \tag{14}$$

$$\psi(\eta) = \frac{[(\gamma+1)/(\gamma-1)]\eta^{3/(\gamma+1)}}{\left[(\gamma+1-\eta^{\beta-1})/\gamma\right]^{(2\gamma+10)/(7-\gamma)}} \tag{15}$$

$$\beta = (7\gamma-1)/(\gamma^2-1) \tag{16}$$

$$T(\eta) = A^2 R^{-3} T_0 \rho_0 f(\eta)/[\gamma P_0 \psi(\eta)] \tag{17}$$

The previous eleven equations define the behavior and thermodynamic state of the gaseous flow after the explosion.

D. Friedman's Blast Wave Solution

The second blast wave solution modeled in the algorithm was developed by Friedman. This solution produces position, velocity, pressure, density, and temperature profiles of the explosive gasses and shock wave. The solution was derived by a spatial modification of a pressurized, one-dimensional shock tube and applied to a much larger explosion. This solution differs from Taylor's in that it uses pressure as opposed to blast wave energy to quantify the initial strength of the explosion. Friedman's solution also incorporates the method of characteristics in its derivation.[13]

An important quantity to be calculated is the shock wave velocity at the instant of the explosion. This quantity is computed by solving for the thermodynamic variables in a one-dimensional shock tube with appropriate pressure and density conditions. Solving Eq. (19) iteratively provides the solution for the initial Mach number of the radiating shock wave, labeled *M*.[13] For simplicity, δ is defined in Eq. (18) and is a function of the ratio of specific heat of the gas phase. The subscript zero refers to the ambient conditions, four refers to the conditions inside the detonated explosive, and *i* refers to the initial time condition.

$$\delta = (\gamma-1)/(\gamma+1) \tag{18}$$

$$\frac{P_4}{P_0}\left\{1-\frac{\delta a_0}{a_4}(M_i - M_i^{-1})\right\}^{(\delta+1)/\delta} = (1+\delta)M_i^{\,2} - \delta \tag{19}$$

Unlike a one-dimensional shock tube where the shock wave Mach number stays constant over time, the shock wave from a spherical explosion will dampen significantly. Friedman accounts for this slowing of the shock wave with a spatial correction factor that reduces to Eq. (20) shown below.[13] The subscript, *s*, refers to the shock wave.

$$-2\frac{dx_s}{x_s} = dM\left\{\frac{4M}{2\gamma M^2-\gamma+1} + \frac{2(M^2+1)}{M\sqrt{[2\gamma M^2-\gamma+1][M^2(\gamma-1)+2]}}\right.$$

$$\left. + \frac{2M}{M^2-1}\sqrt{\frac{(\lambda-1)M^2+2}{2\gamma M^2-\gamma+1}} + \frac{M^2+1}{M(M^2-1)}\right\} \tag{20}$$

The shock wave position and velocity information over time allows the calculation of gas phase velocity, pressure, density, and speed of sound directly behind the shock using the Rankine-Hugoniot relations shown in Eqs. (21), (22), (23), and (24).[13,15,16] All of the following thermodynamic states remain constant in the flow between the shock wave and the advancing front for the explosive gas.

$$v_g = \frac{2a_0}{\gamma+1}(M - M^{-1}) \tag{21}$$

$$P = \frac{P_0}{\gamma+1}(2\gamma M^2 - \gamma + 1) \tag{22}$$

$$\rho = \frac{\rho_0(\gamma+1)M^2}{(\gamma-1)M^2+2} \tag{23}$$

$$a^2 = \frac{{a_0}^2(2\gamma M^2 - \gamma + 1)[M^2(\gamma-1)+2]}{(\gamma+1)^2 M^2} \tag{24}$$

The border between the advancing front of the gaseous detonation products and the surrounding air is referred to as the contact discontinuity. It is important to determine the location of the contact discontinuity because at that point temperature, density, and entropy experience an abrupt change even though pressure and flow velocity remain constant. Being dependent on shock wave position and Mach number, the contact discontinuity position over time is calculated with Eqs. (25) and (26).[13] Eqs. (27) and (28) define *w* and *Q* which are variables used in the method of characteristics. The subscript, *c*, refers to the contact discontinuity while the primes represent differentiation with respect to Mach number.

$$\frac{dt_c}{dM} = \left\{1 + \left(\frac{2}{\gamma-1}\right)\frac{a_{i4}}{a_{i0}}\right\}\{x'_s + w'(t_c - t_s) - wt_s'\}/(2Q - w) \tag{25}$$

$$x_c = x_s + w(t_c - t_s) \tag{26}$$

$$w = v_g - a \tag{27}$$

$$Q = a/(\gamma-1) + v_g/2 \tag{28}$$

Another important aspect of the explosion to model is what happens to the flow inside the sphere as the high pressure gas starts to travel outward. When this happens, an inward moving expansion wave is created where gas velocity, speed of sound, pressure, density, and temperature vary continuously. The algorithm computes these quantities in a similar manner to a pressurized shock tube using Eqs. (29) through (33) shown below.[14,16,17]

Combined, these equations represent another way to define the behavior and flow of the gaseous detonation products. The Friedman blast wave solution is based on a variety of different assumptions and methods as compared to the Taylor blast wave solution and thus produces significantly different results.

$$v_g = \frac{2}{\gamma+1}\left(a_4 + \frac{x}{t}\right) \tag{29}$$

$$\frac{a}{a_4} = 1 - \frac{\gamma-1}{2}\left(\frac{v_g}{a_4}\right) \tag{30}$$

$$\frac{T}{T_4} = \left[1 - \frac{\gamma - 1}{2}\left(\frac{v_g}{a_4}\right)\right]^2 \tag{31}$$

$$\frac{P}{P_4} = \left[1 - \frac{\gamma - 1}{2}\left(\frac{v_g}{a_4}\right)\right]^{2\gamma/(\gamma-1)} \tag{32}$$

$$\frac{\rho}{\rho_4} = \left[1 - \frac{\gamma - 1}{2}\left(\frac{v_g}{a_4}\right)\right]^{2/(\gamma-1)} \tag{33}$$

E. Energy Coupling

The algorithm also incorporates energy coupling into both the Taylor and Friedman blast wave solutions. When using the Taylor blast wave solution, the change in particle kinetic and thermal energy is subtracted from the blast wave energy for each particle per time step. This results in a general attenuation of the blast wave as the particles drain energy. As time progresses and the increased particle velocities and temperatures approach that of the blast wave, less transfer occurs. Thus, Taylor's blast wave solution must be re-evaluated, accounting for the updated blast wave energy, at each time step in the algorithm.

Since the Friedman blast wave solution is derived from the pressurized one-dimensional shock tube solution, it is necessary to reduce the initial pressure condition in order to model the energy loss from the gaseous flow. Energy loss is determined at each new time step in the algorithm followed by an appropriate reduction of the initial detonation pressure. Like the Taylor solution, the entire Friedman blast wave solution must be re-evaluated at each time step in the algorithm to account for energy transfer between the gas phase and solid phase.

F. Particle Tracking

The gas phase and solid phase are tracked using an Eulerian and Lagrangian approach respectively. The gas phase is assumed to be a continuum. Gas flow properties change gradually when using the Taylor method. When using the Friedman method, the flow properties change gradually as well with the exceptions of the abrupt changes occurring at the head of the expansion wave, tail of the expansion wave, and contact discontinuity. Each particle's position, velocity, and temperature is tracked individually in a Lagrangian manner and updated at each time step.

III. Results and Analysis

A. Gurney Velocity Initialization

The results of the Gurney velocity initialization are shown in Fig. 1. Illustrated is increasing velocity from the explosive core to the outer edge of the explosive. Gas near the outer edge of the outer shell experiences less backward pressure and thus achieves a higher initial velocity. Particle velocities are slower than gas velocities at each point due to the fact that each calculated layer of explosive has only a fraction of surface area made up of particles. Detonated gas escapes between the gaps in the particles which creates the velocity difference shown. This method produces an acceptable input to the algorithm.

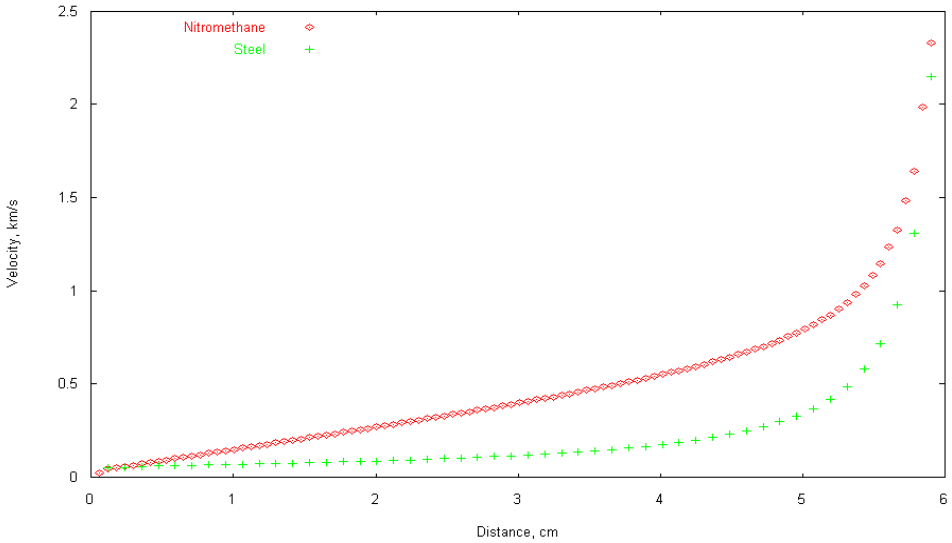

Figure 1. Velocity as a function of radial distance from core.

B. Taylor Method Results

Using Taylor's blast wave solution in the algorithm produces several important results. Figure 2 shows the velocity profile of the gas phase during five different times. Velocity is shown as a function of radial distance from the core of the explosive. The velocity profile shows no abrupt changes and attenuates as it expands outward. Figure 3 illustrates the pressure profile for the gas phase for equivalent times in the simulation. Taylor's method predicts a spike in pressure near the edge of the propagating explosive gas which is produced by the algorithm.

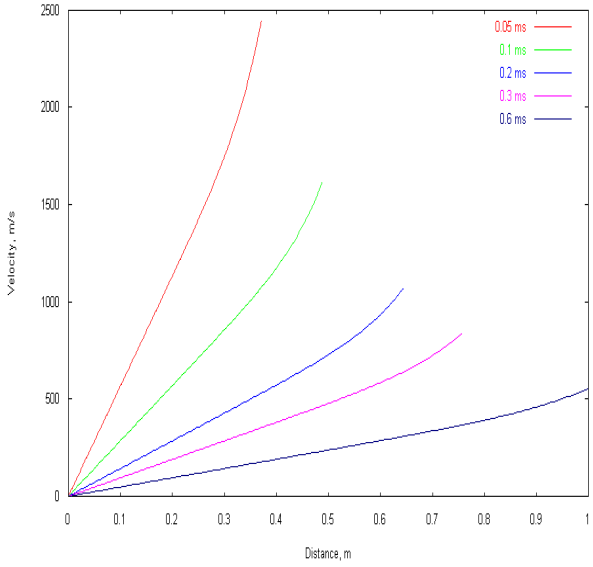

Figure 2. Gas velocity as a function of distance.

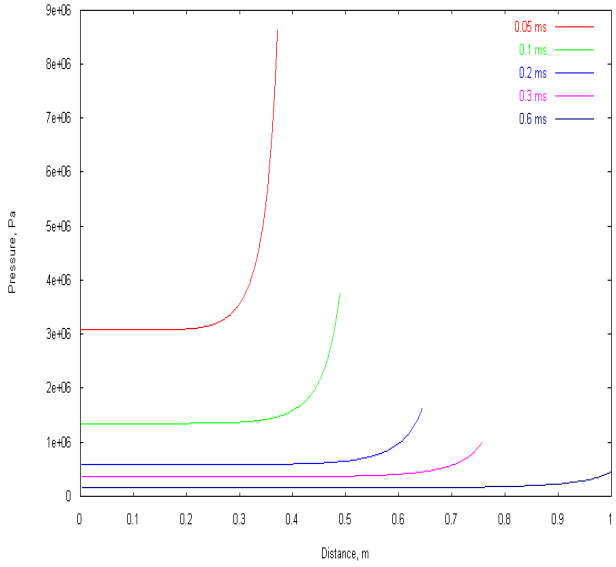

Figure 3. Gas pressure as a function of distance.

Figure 4 plots the temperature of the gas phase as a function of radial distance. This result clearly illustrates one of the limitations associated with using the Taylor method, i.e., temperatures near the core are far too high. The primary reason for this difficulty is that the derivation of the temperature profile assumes a calorically perfect gas with a constant ratio of specific heats. This assumption is less valid near the core of the explosive where the ratio of specific heats changes dramatically. Near the outer edge of the gas flow, a calorically perfect gas is more accurate and yields more accurate temperature results.

Figure 5 displays gas density as a function of distance from the core over various times. The density profile is similar to that of the pressure profile. This physically means that the bulk of the gaseous detonation products propagate outward in a dense high pressure shell. This result shows another limitation for the Taylor blast wave solution resulting from the assumption that the entire explosive has radiated outward starting from a very small source. The algorithm compensates by initializing the blast radius at the same size as the explosive sphere. Nevertheless, the assumption of a very small source at the initial time significantly affects the results of the density and pressure profiles.

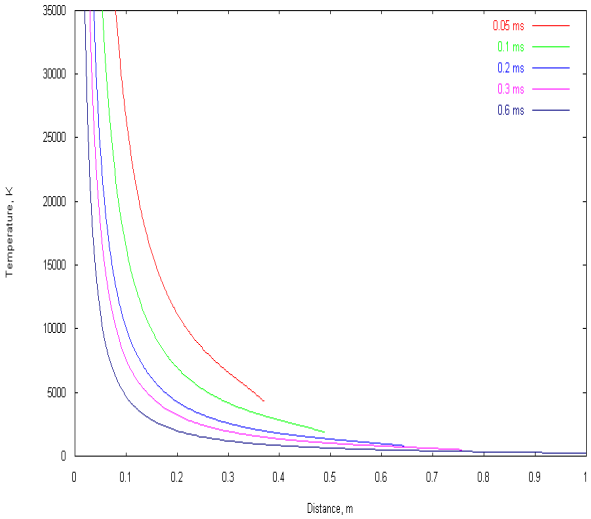

Figure 4. Gas temperature as a function of distance.

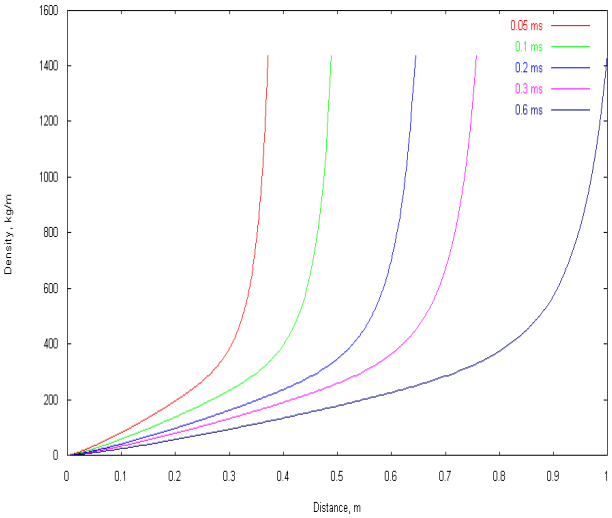

Figure 5. Gas density as a function of distance.

Figures 6 and 7 show the results of the solid phase using Taylor's method. In Fig. 6, particle velocity is slow near the core of the explosive and higher near the outer edge. All particles slow over time as they travel outward. From Fig. 7, it can be seen that the particles heat rapidly soon after detonation and then gradually cool. The inaccuracy in the calorically perfect gas model can be seen from these results as well. Several particles achieve much greater temperatures than expected near the core.

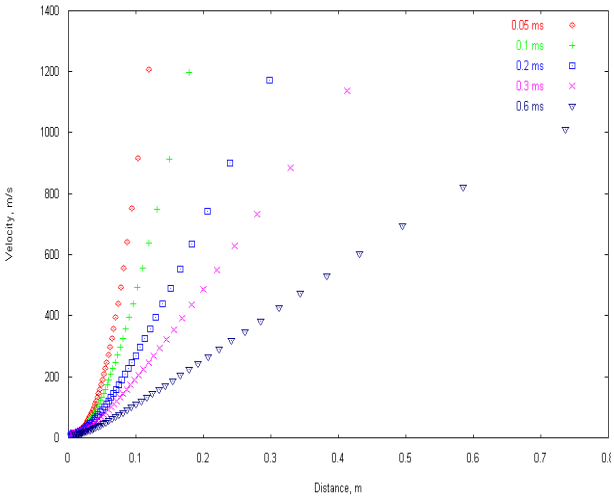

Figure 6. Particle velocity as a function of distance.

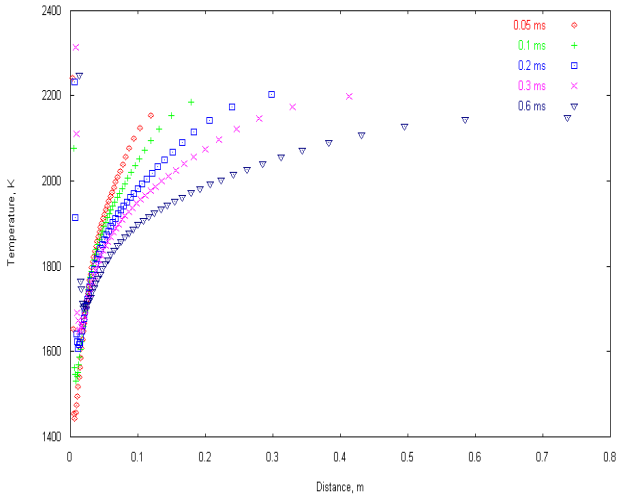

Figure 7. Particle temperature as a function of distance.

The validity of the algorithm can be judged by comparison with the Frost data.[6] Figures 8 and 9 show an overlay of trajectory plots created by the algorithm as well as experimental data measured by Frost. Figure 8 graphs the leading edge of the gas phase and leading particles sized at 463 micrometers in diameter. Figure 9 shows the results using 925 micrometer diameter particles. All results use nitromethane as the high explosive.

A crossing of the trajectories is shown on both graphs. Physically, this represents how the particles gradually outrun the shock wave. The particles accelerate during the initial detonation and then accelerate further within the resulting blast wave flow. Over time, the particles gain velocity and momentum while the shock wave starts to dampen out. This effect is observed in both the algorithm as well as experiment.

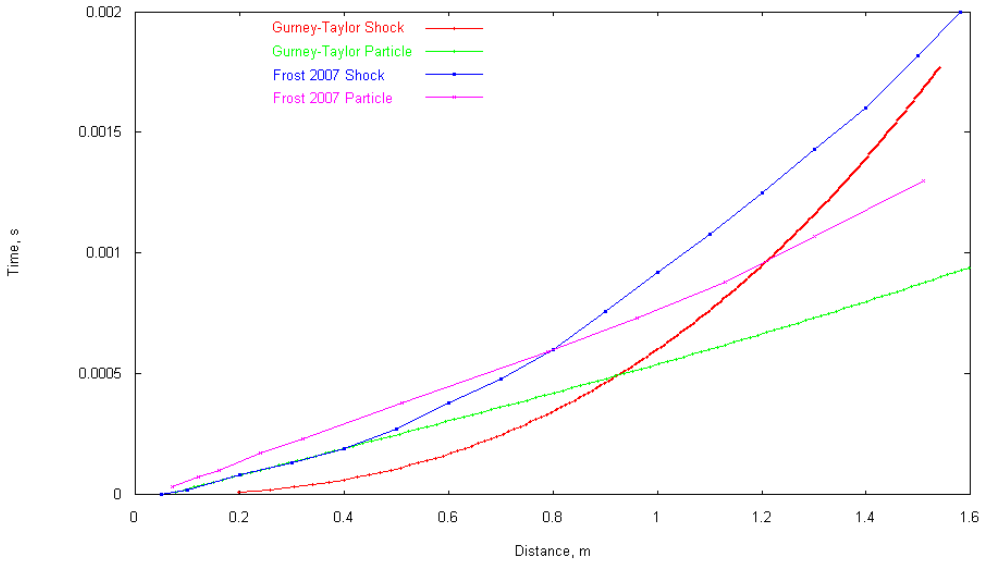

Figure 8. Time versus distance trajectory plot including Frost data for 463 micrometer particles.

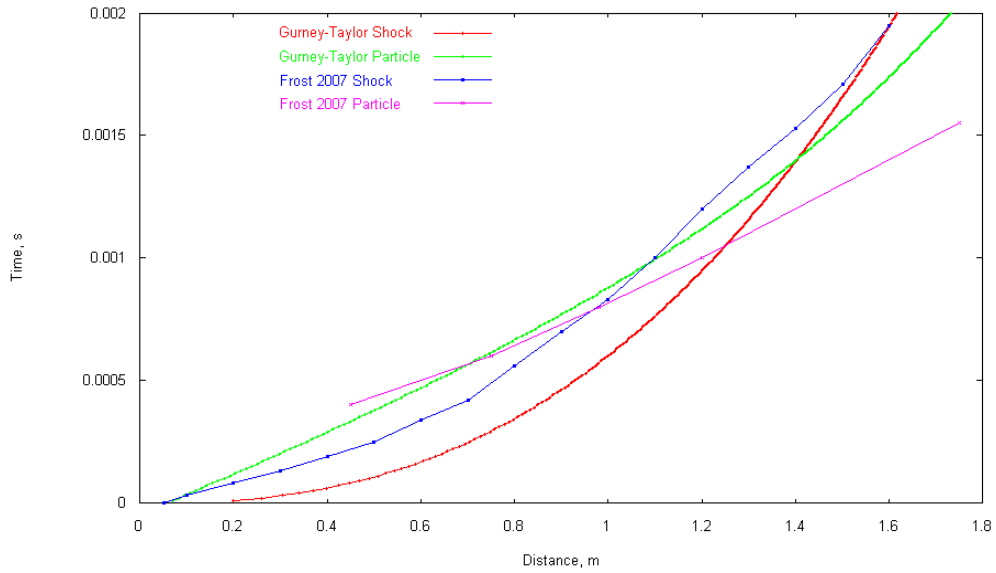

Figure 9. Time versus distance trajectory plot including Frost data for 925 micrometer particles.

C. Friedman Method Results

Using Friedman's blast wave solution in the algorithm produces distinctly different results than the Taylor method. Because this method analyzes specific sections of flow separately, there are discontinuous thermodynamic variables. Velocity is shown in Fig. 10 to have a distinct spike toward the outer shell and gradually slow near the core. Pressure is maintained near the core of the explosive rather than accumulating near the outer edge of the propagating sphere displayed in Fig. 11 in a more accurate representation of the flow.

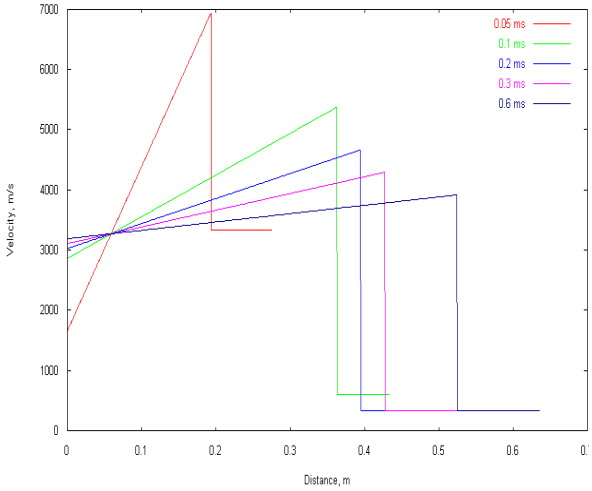

Figure 10. Gas velocity as a function of distance.

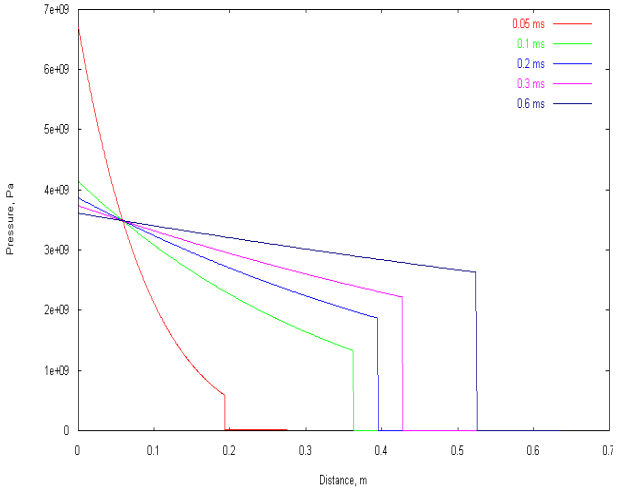

Figure 11. Gas pressure as a function of distance.

The temperature of the gas phase is dramatically different with Friedman's solution than Taylor's. The gas can be seen in Fig. 12 to be less hot near the core and cools much less significantly with radial distance. There is no asymptotic increase in temperature near the core as there was with the Taylor solution. Temperature is also shown to be higher in the expansion wave than in the rest of the flow. Gas density is seen to be high near the core in the expansion wave and gradually decreases with radial distance as shown in Fig. 13.

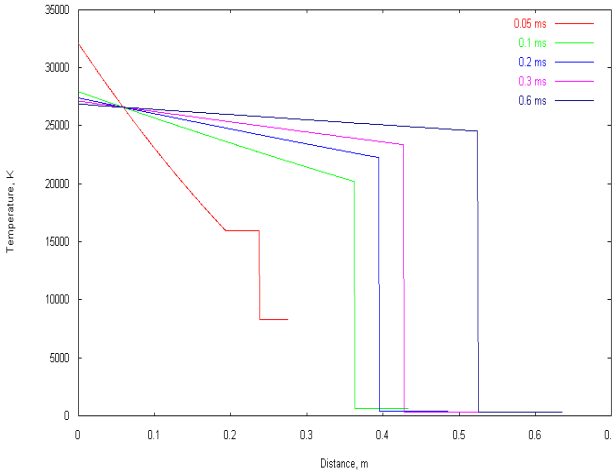

Figure 12. Gas temperature as a function of distance.

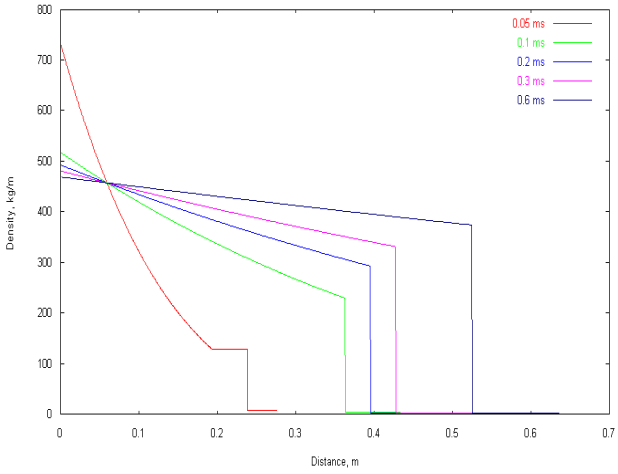

Figure 13. Density as a function of distance.

The solid phase shows expected results. The particles accelerate very rapidly early in the simulation due to the initial detonation acceleration and blast wave flow but slow due to drag illustrated in Fig. 14. Figure 15 shows that the particles initially heat in the expansion wave but then cool as they propagate outward. There are no abnormally hot particles near the core using the Friedman blast wave solution.

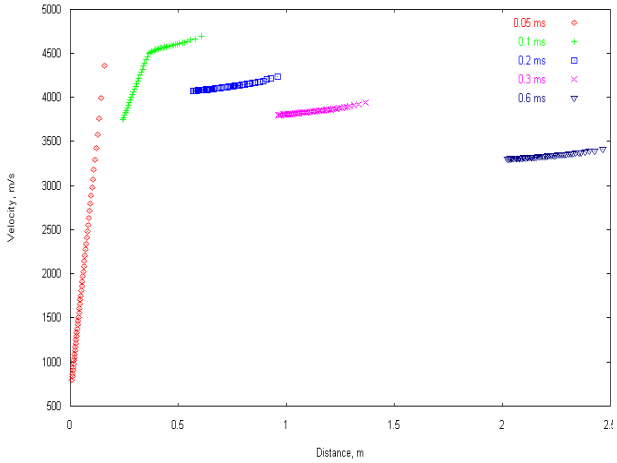

Figure 14. Particle velocity as a function of distance.

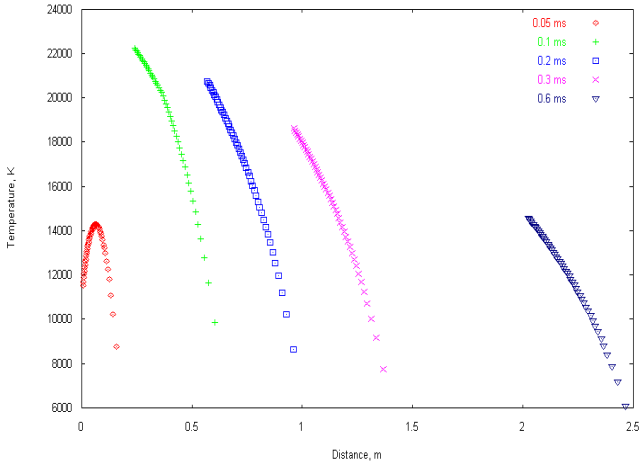

Figure 15. Particle temperature as a function of distance.

Figures 16 and 17 show trajectory plots along with the data from the Frost experiment.[6] In this case, the Friedman blast wave solution produces less accurate results than the Taylor blast wave solution. Here, the shock wave propagates far too quickly at the beginning of the simulation and thus propels the particles to an unusually high velocity. The point where the particles outrun the shock occurs too early in time as well as to close to the core. The trajectory plots expose an inaccuracy in using the Friedman blast wave solution even though the more intricate nature of the flow is captured compared to the Taylor solution.

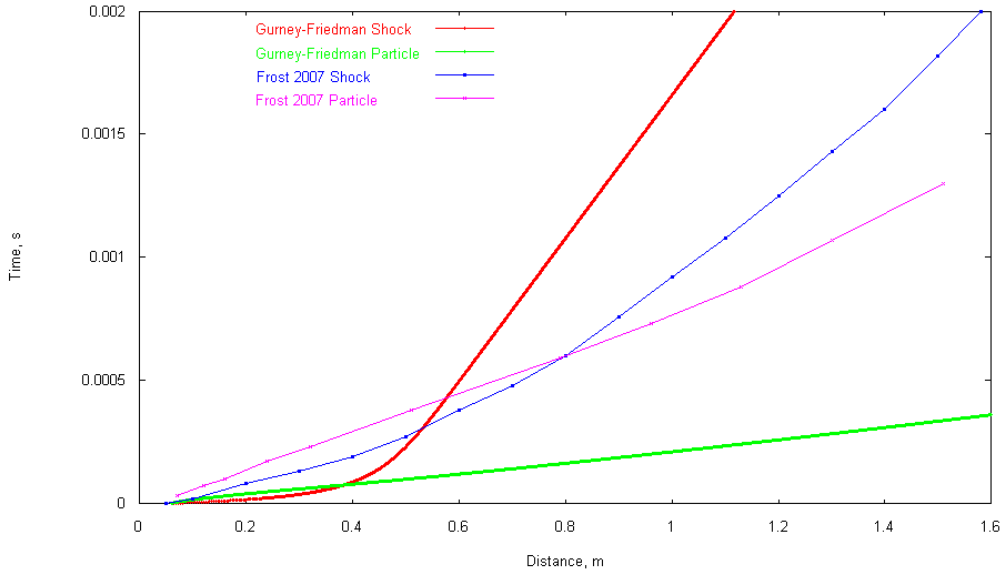

Figure 16. Time versus distance trajectory plot including Frost data for 463 micrometer particles.

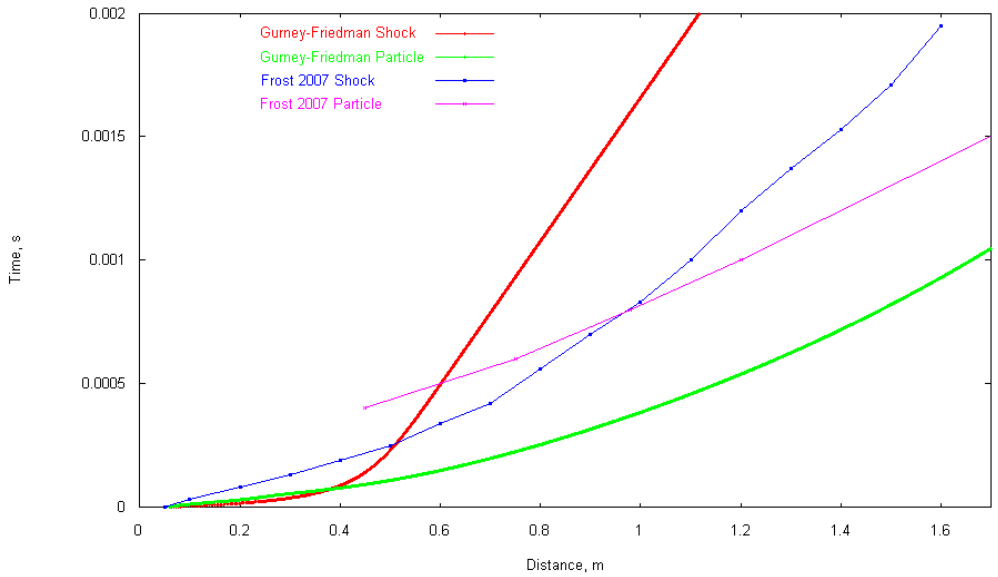

Figure 17. Time versus distance trajectory plot including Frost data for 925 micrometer particles.

IV. Conclusion

This algorithm has modeled a heterogeneous high explosive by combining a velocity initialization scheme, appropriate drag and heat transfer laws, two different blast wave profiles, kinetic and thermal energy coupling, and a Lagrangian-Eulerian tracking scheme. One of the significant limitations to this model is the assumption that the detonation products act as a calorically perfect gas. To refine the algorithm, it is suggested to model a thermally perfect gas which accounts for a changing ratio of specific heats. The Taylor blast wave solution is also limited by its assumption that the radiating gas products are compressed to a small point at the initial time. Still, Taylor's use of a more general blast wave energy quantization allows the method to produce reasonably accurate results. The Friedman blast wave solution does capture more details of the blast wave flow; however it produces less accurate results displayed by its trajectory plots. One reason for the inaccuracy while using the Friedman blast wave solution is that while the expansion wave, shock wave, and contact discontinuity are modeled correctly, flow properties at later times require additional modeling. For example, when the expansion wave reaches the core of the explosive, in reality a reflected wave would be generated. This is not accounted for in Friedman's analysis. Friedman's solution was not based on the extremely high pressures commonly occurring in the detonation of high explosives. We plan to continue improving our implementation of the algorithms as time permits. Still, both solutions used in the algorithm provide insight into the behavior of heterogeneous high explosives.

Acknowledgments

C. M. Engelhardt thanks Dr. Doug Nance for his guidance and support.

References

[1]Baer, M. R., and Nunziato, J. W., "A Two-Phase Mixture Theory for the Deflagration-to-Detonation Transition (DDT) in Reactive Granular Materials," *International Journal of Multiphase Flow*, Vol.12, No. 6, 1986, pp. 861-889.

[2]Lanovets, V. S., Levich, V. A., Rogov, N. K., Tunik, Y. V., and Shamshev, K. N., "Dispersion of the Detonation Products of a Condensed Explosive with Solid Inclusions," *Combustion, Explosion, and Shock Waves*, Vol. 29, No. 5, 1994, pp. 638-641.

[3]Patankar, N. A., and Joseph, D. D., "Modeling and numerical simulation of particulate flows by the Eulerian-Lagrangian approach," *International Journal of Multiphase Flow*, Vol. 27, 2001, pp. 1659-1684.

[4]Powers, J. M., "Two-phase viscous modeling of compaction of granular materials," *Physics of Fluids*, Vol. 16, No. 8, 2004, pp. 2975-2990.

[5]Meyers, M., *Dynamic Behavior of Materials*, John Wiley & Sons, Inc., New York, 1994, Chap. 9.

[6]Frost, D. L., Ornthanalai, C., Zarei, Z., Tanguay, V., and Zhang, F., "Particle momentum effects from the detonation of heterogeneous explosives," *Journal of Applied Physics*, Vol. 101, No. 113529, 2007.

[7]Zhang, F., Frost, D. L., Thibault, P. A., and Murray, S. B., "Explosive dispersal of solid particles," *Shock Waves*, Vol. 10, 2001, pp 431-443.

[8]Akhatov, I. S., and Vainshtein, P. B., "Transition of Porous Explosive Combustion into Detonation," *Combustion, Explosion, and Shock Waves*, Vol. 20, No. 1, 1984, pp.63-70.

[9]Nance, D., "Velocity Extrema for Fragments Propelled by the Explosion of a Cylindrical Warhead," Technical Report, Munitions Directorate, Air Force Research Laboratory, 2007.

[10]Nance, D., "Blast Wave Initial Conditions for LES3D, Part I – Practical Instructions for the Solution Initialization Coding," Technical Memorandum, Munitions Directorate, Air Force Research Laboratory, 2005.

[11]Nance, D., "Improved Initial Conditions for Particle-Laden Blast Waves," Technical Memorandum, Munitions Directorate, Air Force Research Laboratory, 2005.

[12]Taylor, G., "The formation of a blast wave by a very intense explosion I. Theoretical discussion," *Proc. Roy. Soc. A*, Vol. 201, 1950, pp. 159-174.

[13]Friedman, M. P., "A Simplified Analysis of Spherical and Cylindrical Blast Waves," Aerophysics Laboratory, Massachusetts Institute of Technology, 1961.

[14]Sachdev, P. L., *Shock Waves and Explosions*, Chapman & Hall, New York, 2004, Chap. 7.

[15]Zukas, J. A., and Walters, W. P. Eds., *Explosive Effects and Applications*, Springer-Verlag, New York, 1998.

[16]Anderson, J. D., *Modern Compressible Flow with Historical Perspective*, 2nd ed., McGraw-Hill, Inc., New York, 1990, Chap. 7.

[17]Hirsch, C., *Numerical Computation of Internal and External Flows Volume 2: Computational Methods for Inviscid and Viscous Flows*, John Wiley & Sons Ltd., Chichester, England, UK, 1990, Chap. 16.

Numerical Modeling of Heterogeneous High Explosives

40th AIAA Thermophysics Conference
23 June 2008

1Lt Chris Engelhardt

Munitions Directorate

Air Force Research Laboratory

Eglin AFB, FL

Introduction

- **Purpose**
  - To develop and test an accurate multiphase blast explosive model
  - Research results of Gurney initialization scheme
- **Objectives**
  - Incorporate Gurney method initialization
  - Test various drag laws
  - Test various heat transfer laws
  - Model Taylor and Friedman Blast Wave solutions
  - Examine energy coupling
  - Compare to experiment

Background

- Taylor versus Friedman blast wave solutions
- Gurney method approximates particle velocities for outer shell fragments
- “Spray” drag law, Carlson and Hoglund rocket equations, Vainshtein and Akhatov explosion equations
- Frost and Zhang experimental data from 2007

Technical Approach

- Designed numerical algorithm
  - Initialize velocity
  - Determine particle acceleration and temperature change
  - Alter blast wave solution
  - Update particle position and temperature
- Combined different authors' work with most reasonable assumptions
- Compared with experimental data

Gurney Initialization

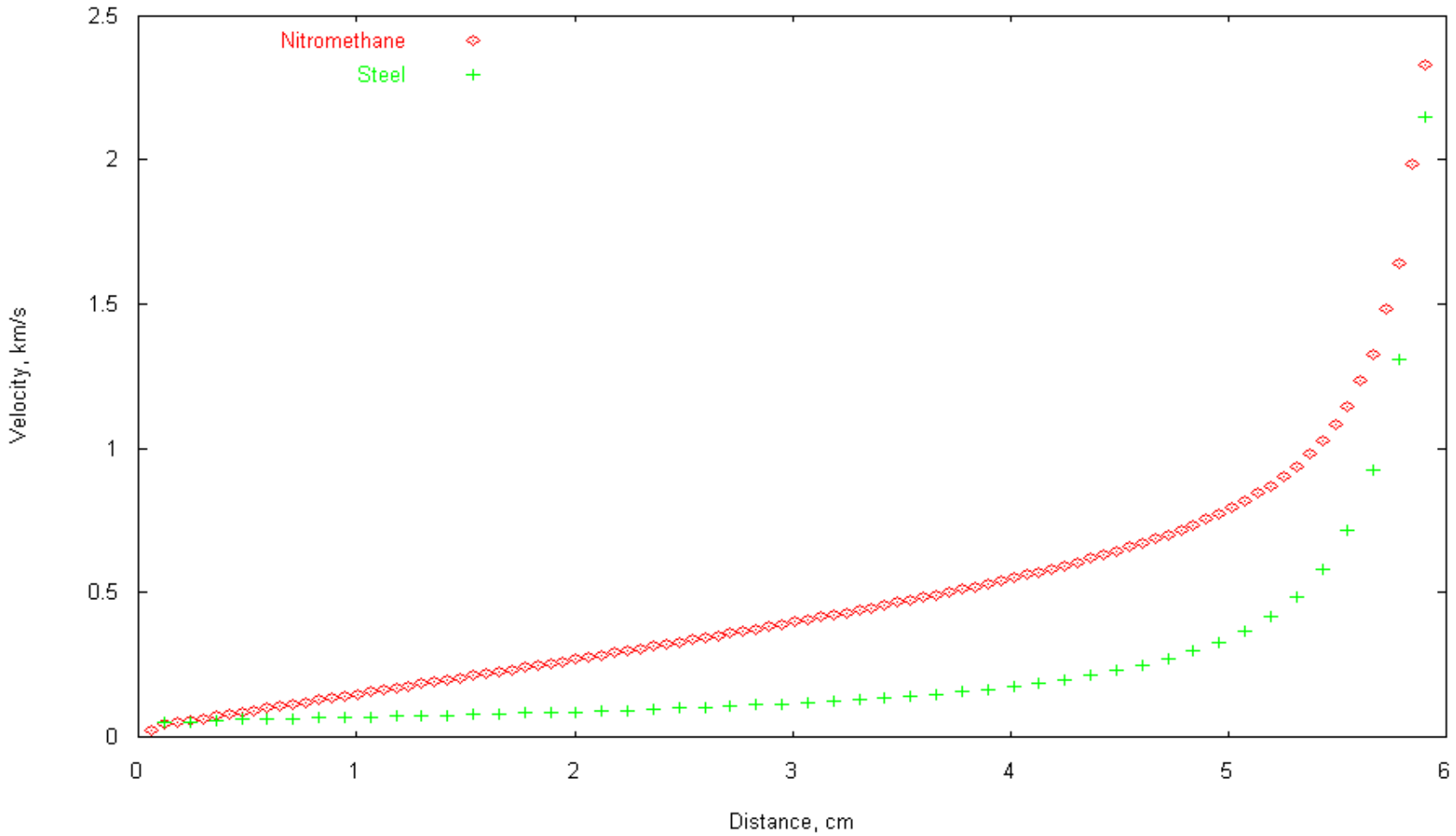

Drag and Temperature

- **Authors Vainshtein and Akhatov**
  - **Force of drag**

$$\mathrm{Re} = \frac{\rho \left| v_g - v_p \right| d}{\mu}$$

$$f = \frac{\pi d^2}{4} C_d \rho \frac{\left| v_g - v_p \right| \left(v_g - v_p \right)}{2}$$

$$C_d = \begin{cases} C_1 = \dfrac{24}{\mathrm{Re}} + \dfrac{4.4}{\mathrm{Re}^{0.5}} + 0.42 & \alpha_2 \le 0.08 \\ C_2 = \dfrac{4}{3\alpha_1}\left(1.75 + \dfrac{150\alpha_2}{\alpha_1 \mathrm{Re}}\right) & \alpha_2 \ge 0.45 \\ C_3 = \dfrac{\left(\alpha_2 - 0.08\right) C_2 + \left(0.45 - \alpha_2\right) C_1}{0.37} & 0.08 < \alpha_2 < 0.45 \end{cases}$$

  - **Temperature change**

$$\dot{q} = \pi d \lambda N_u \left(T_g - T_p \right) \left(m C_p \right) \qquad N_u = \begin{cases} 2 + 0.106\, \mathrm{Re}\, \mathrm{Pr}^{1/3} \\ 2.274 + 0.6\, \mathrm{Re}^{0.67}\, \mathrm{Pr}^{1/3} \end{cases}$$

Taylor's Governing Equations

- **Pressure** $$\frac{P}{P_0} = \frac{A^2}{a^2} R^{-3} f(\eta)$$
- **Density** $$\frac{\rho}{\rho_0} = \psi(\eta)$$
- **Velocity** $$u = AR^{\frac{-3}{2}} \phi(\eta)$$
- **Blast Radius** $$R(t) = \left(\frac{5}{2} A\right)^{\frac{2}{5}} t^{\frac{2}{5}}$$
- **Temperature** $$T(\eta) = A^2 R^{-3} \frac{T_0 \rho_0}{\gamma P_0} \frac{f(\eta)}{\psi(\eta)}$$

Friedman Method

- Modeled as a perturbed shock tube
- Initial pressure assigned as Chapman-Jouquet pressure
- Rankine-Hugoniot relations for flow behind shock wave
- Method of characteristics used for contact discontinuity
- Shock tube equations for expansion wave

Gas Phase Velocity

- **Taylor solution**

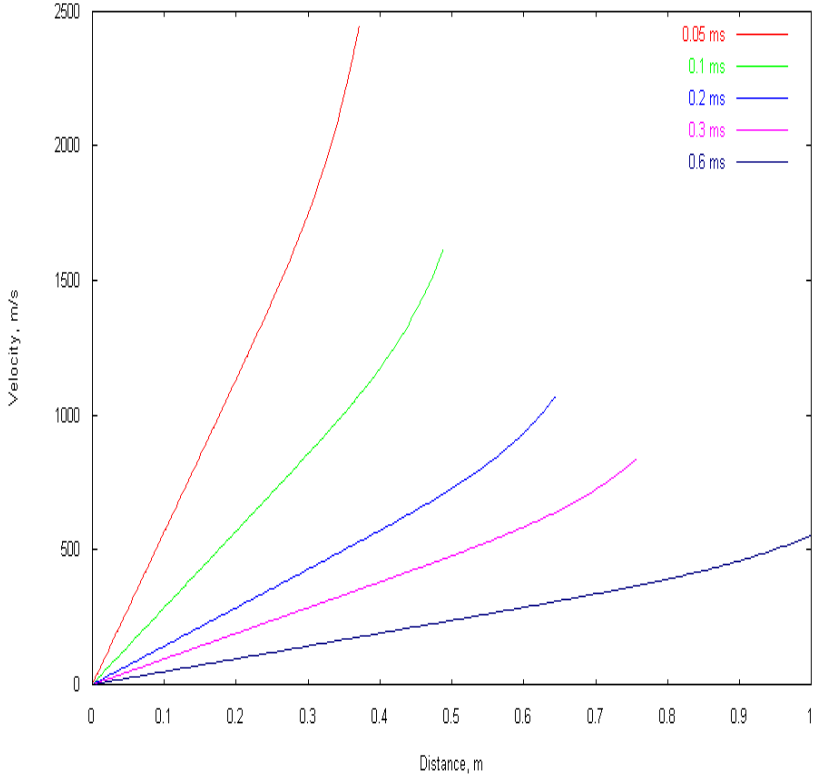

- **Friedman solution**

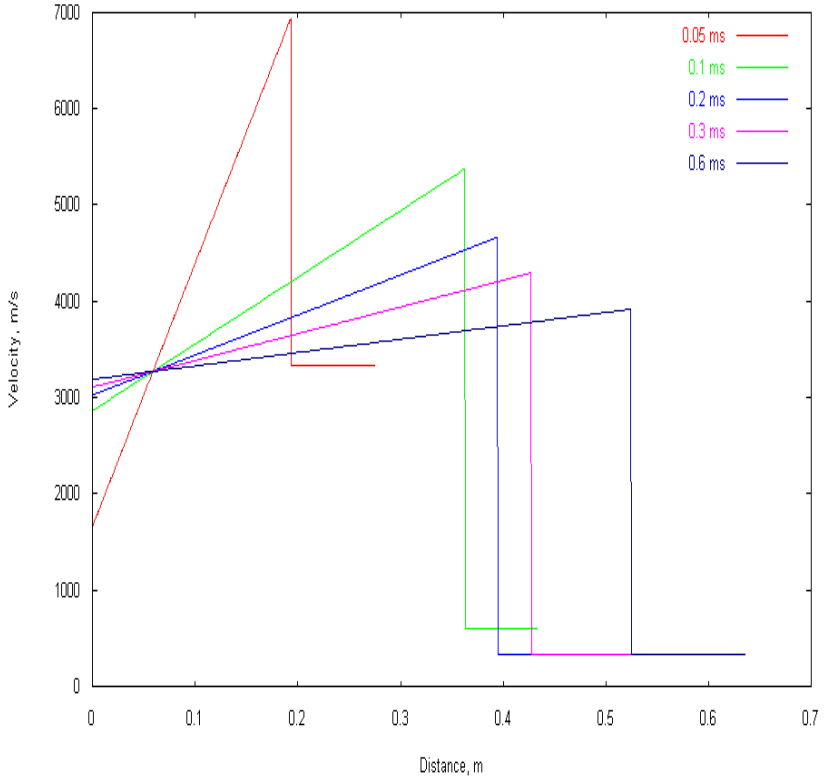

Gas Phase Density

- **Taylor solution**

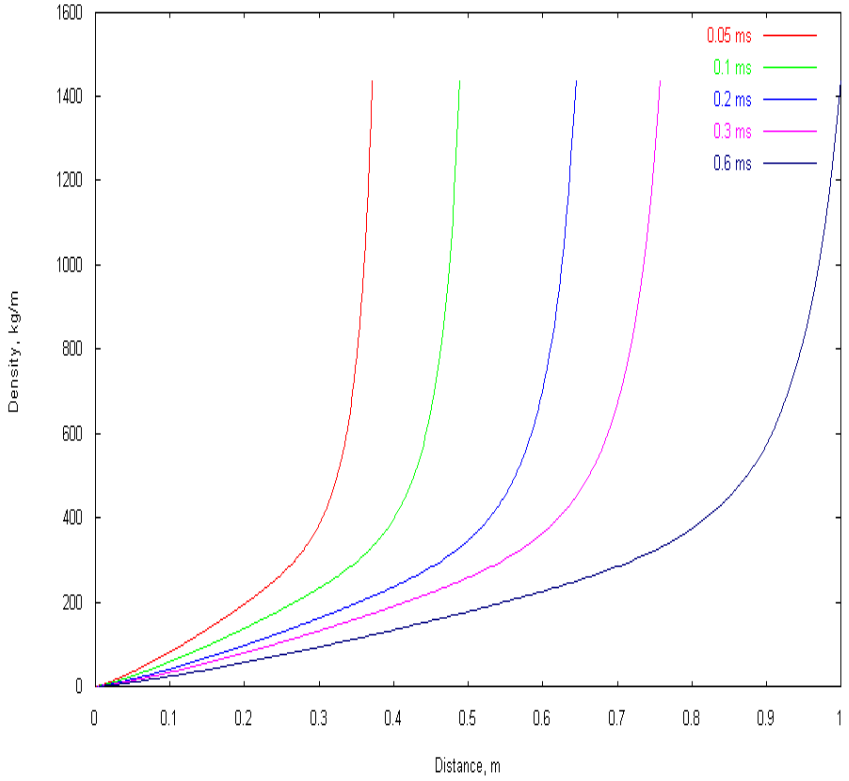

- **Friedman Solution**

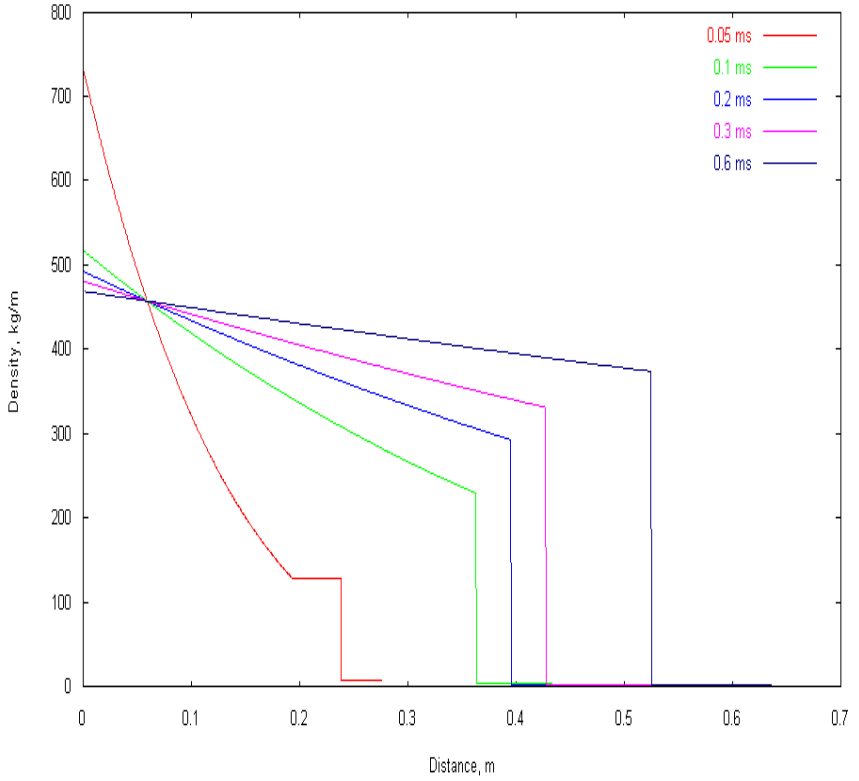

Gas Phase Pressure

- **Taylor solution**

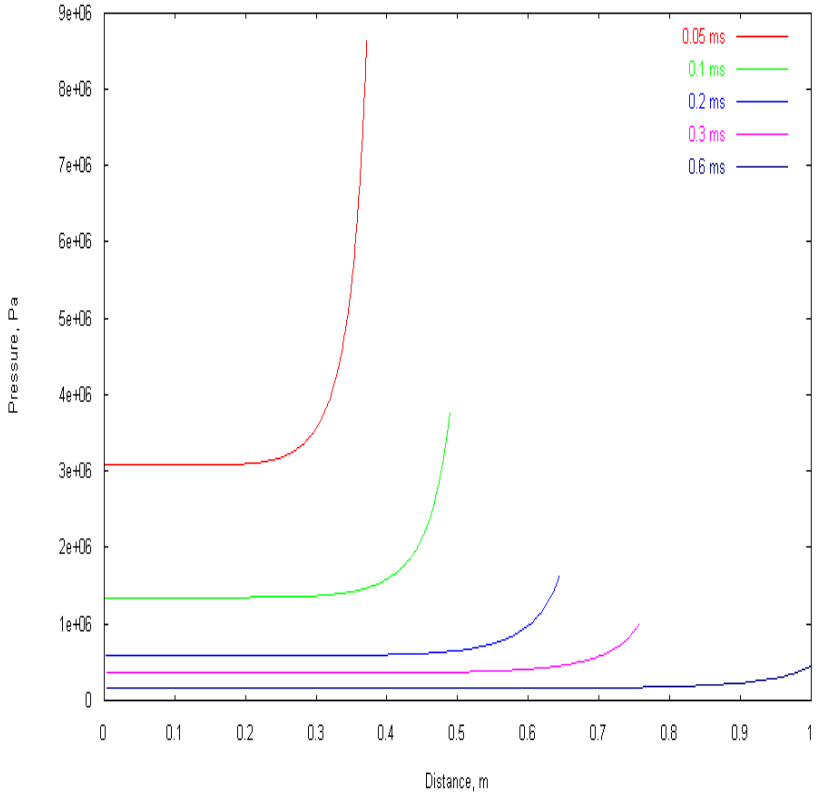

- **Friedman solution**

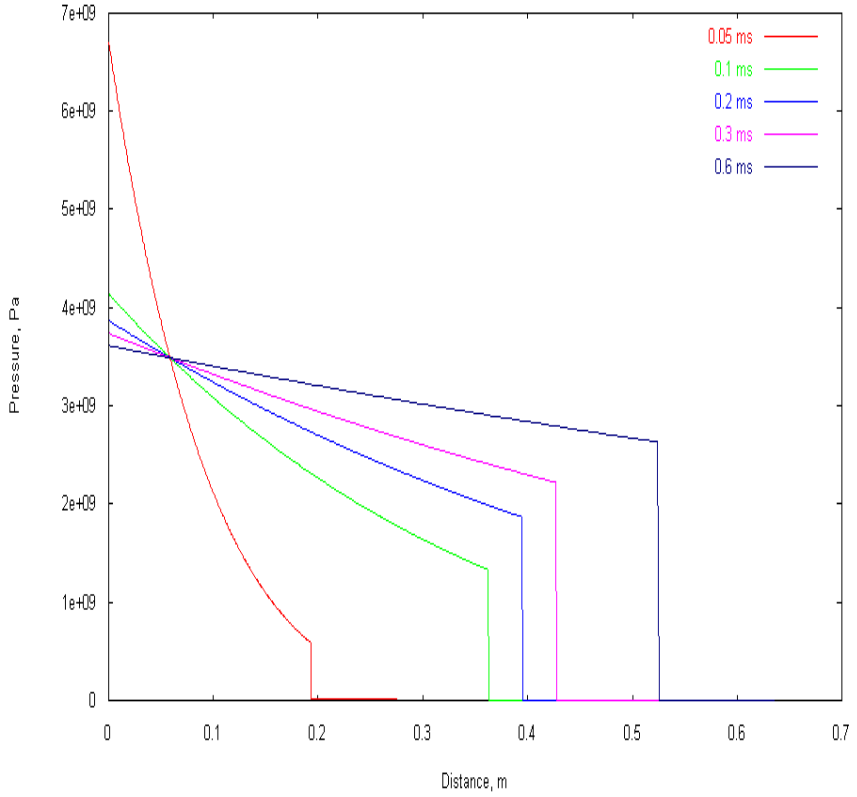

Gas Phase Temperature

- **Taylor solution**

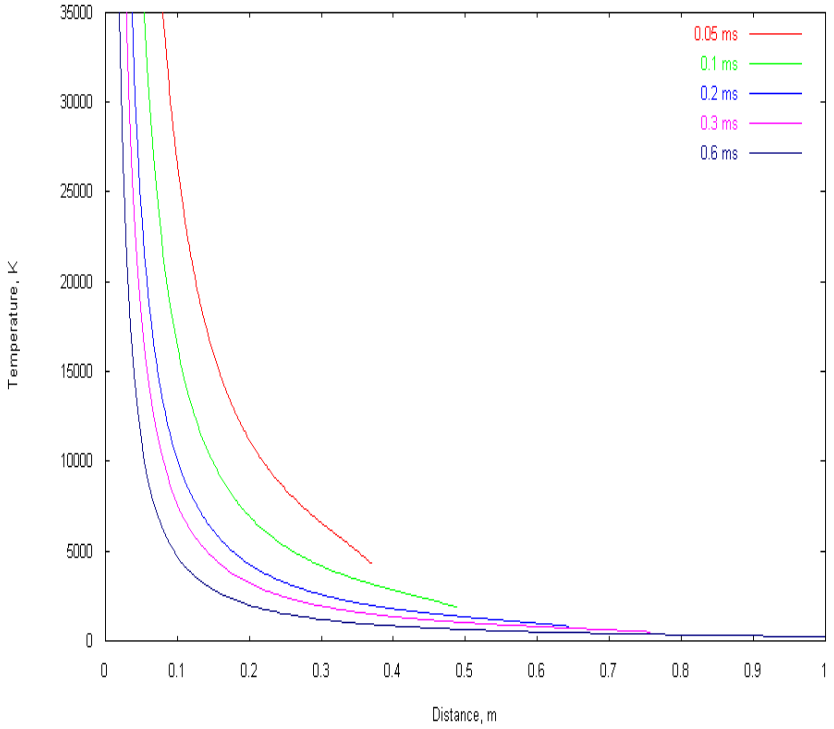

- **Friedman solution**

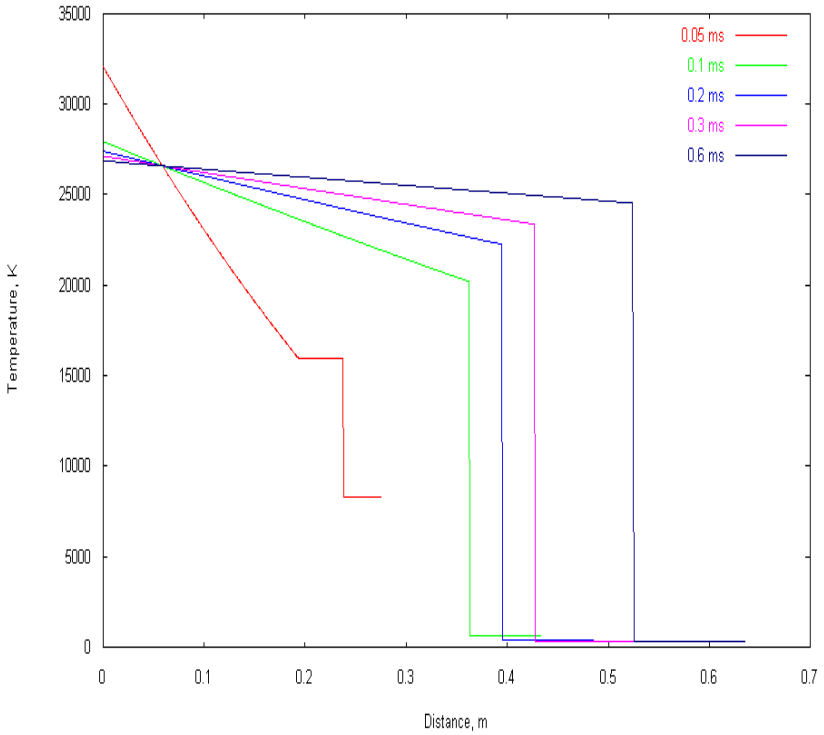

Solid Phase Velocity

- **Taylor solution**

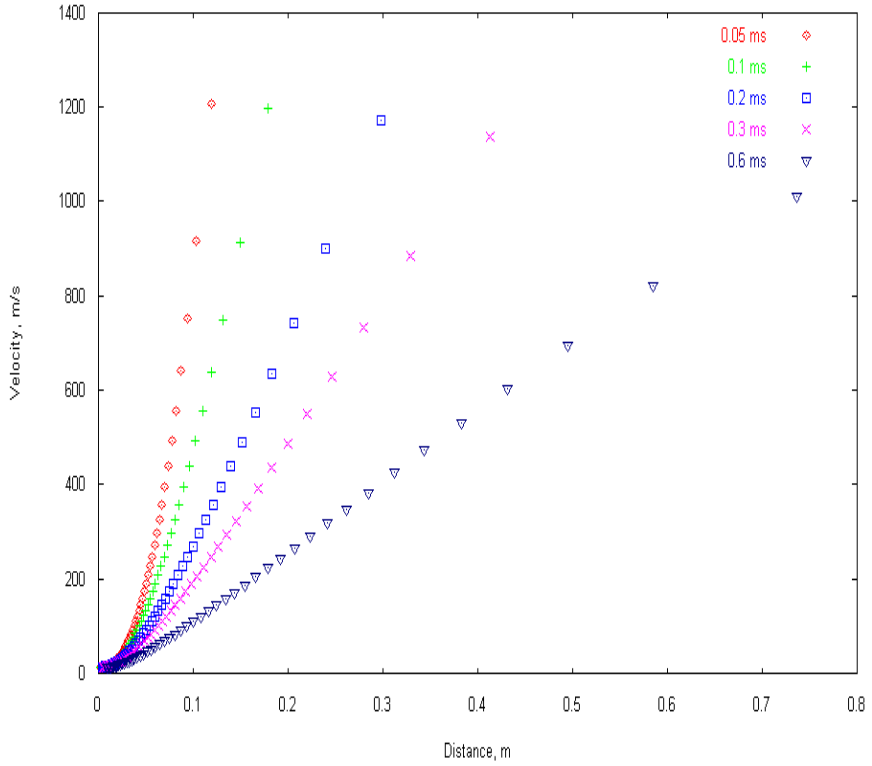

- **Friedman solution**

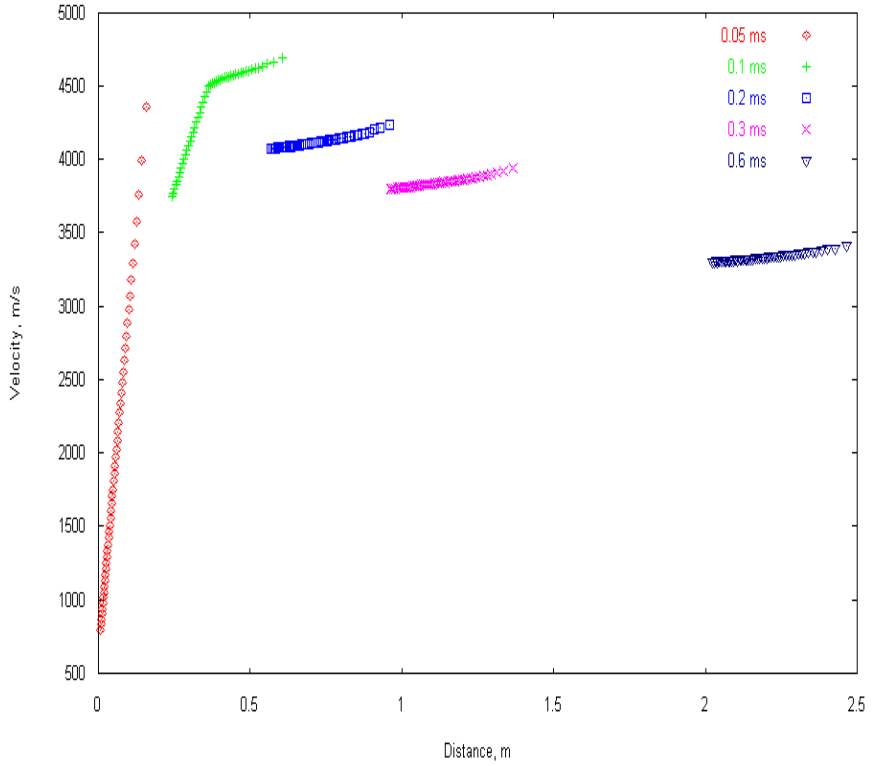

Solid Phase Temperature

- Taylor solution

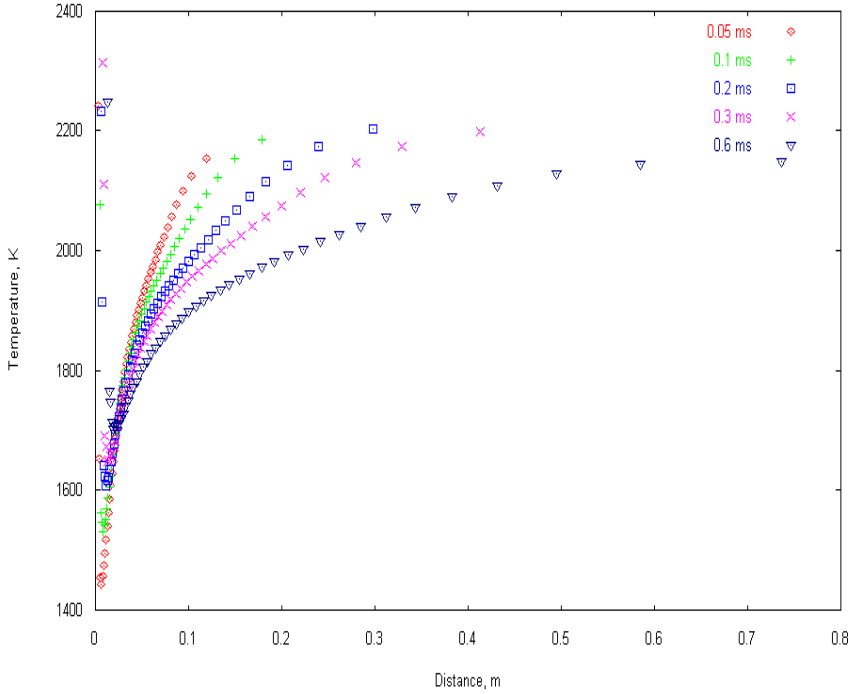

- Friedman solution

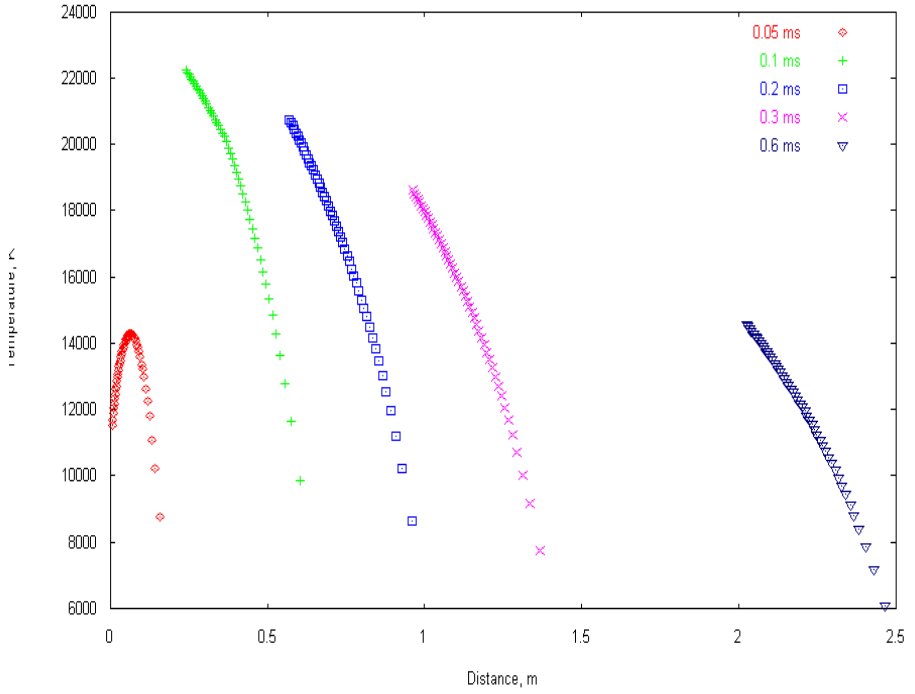

Trajectory Results
463 micrometer particles

- **Taylor solution**

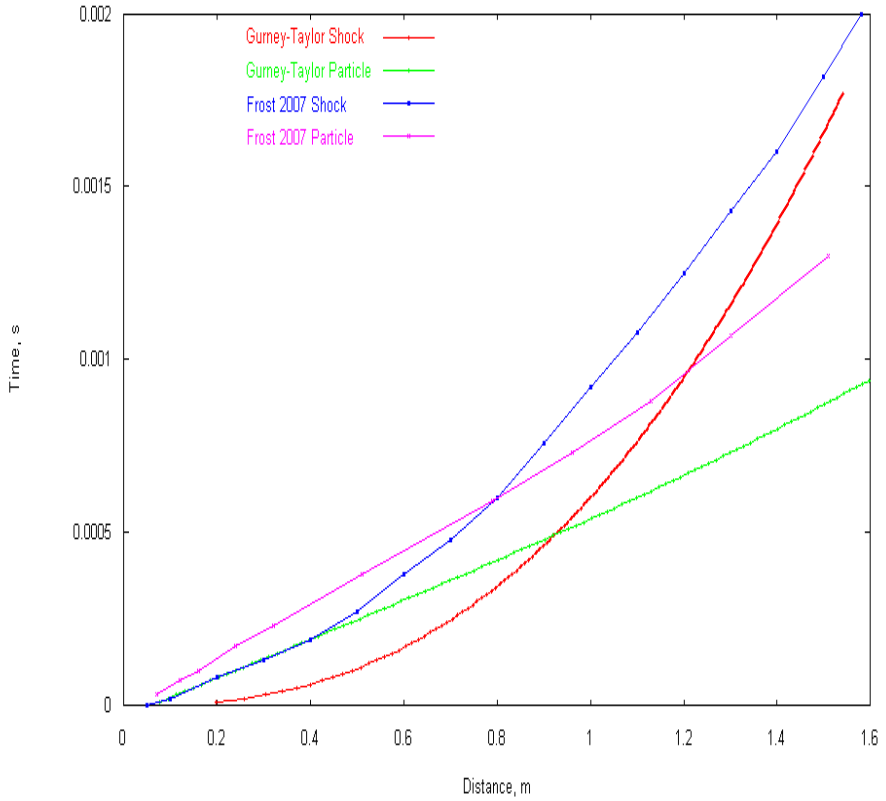

- **Friedman solution**

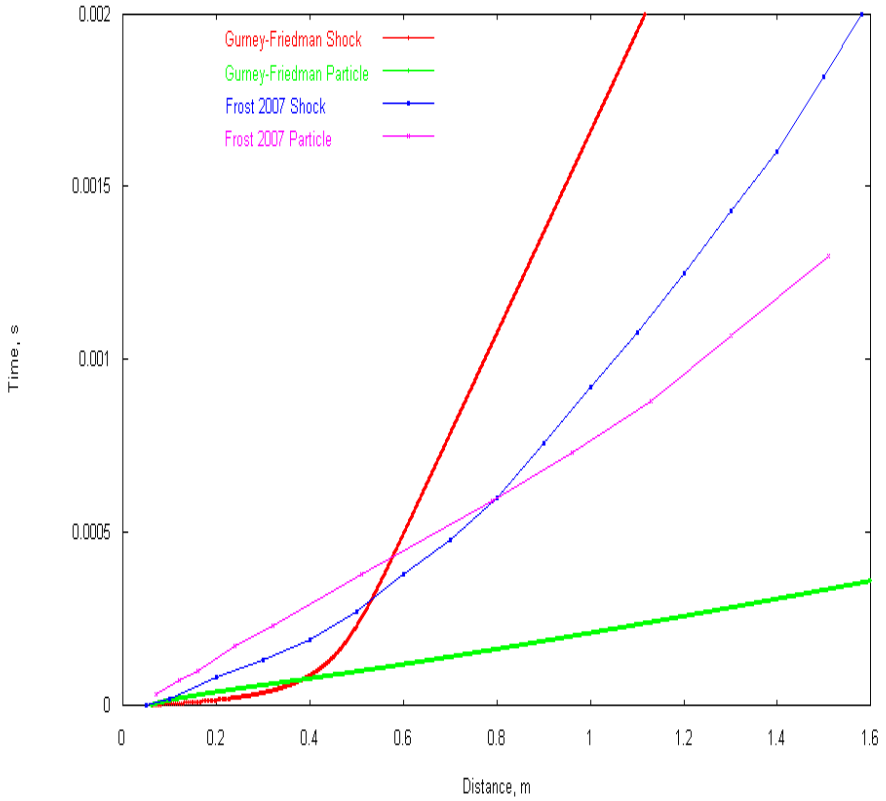

Trajectory Results
925 micrometer particles

- **Taylor solution**

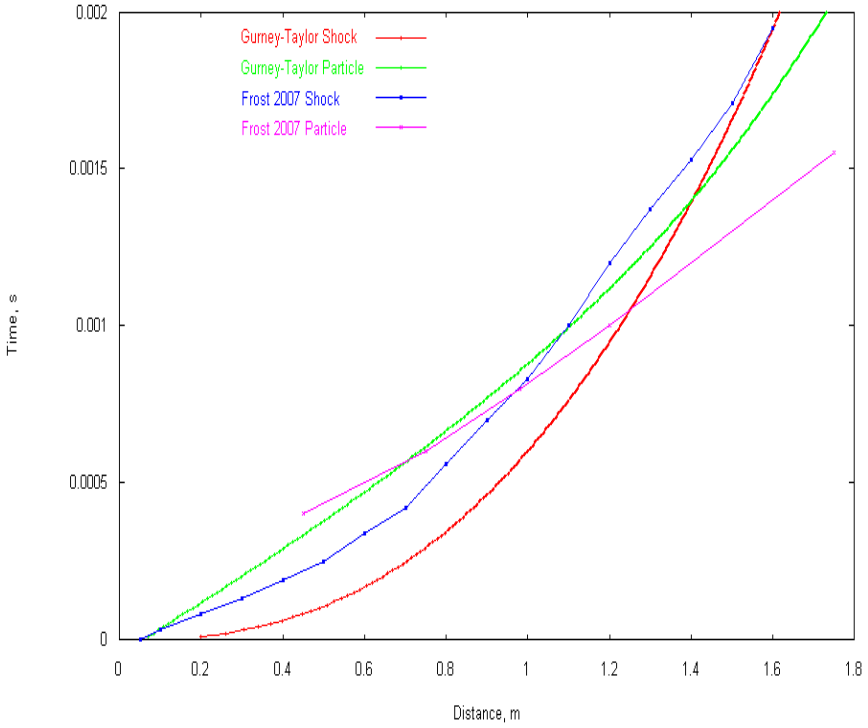

- **Friedman solution**

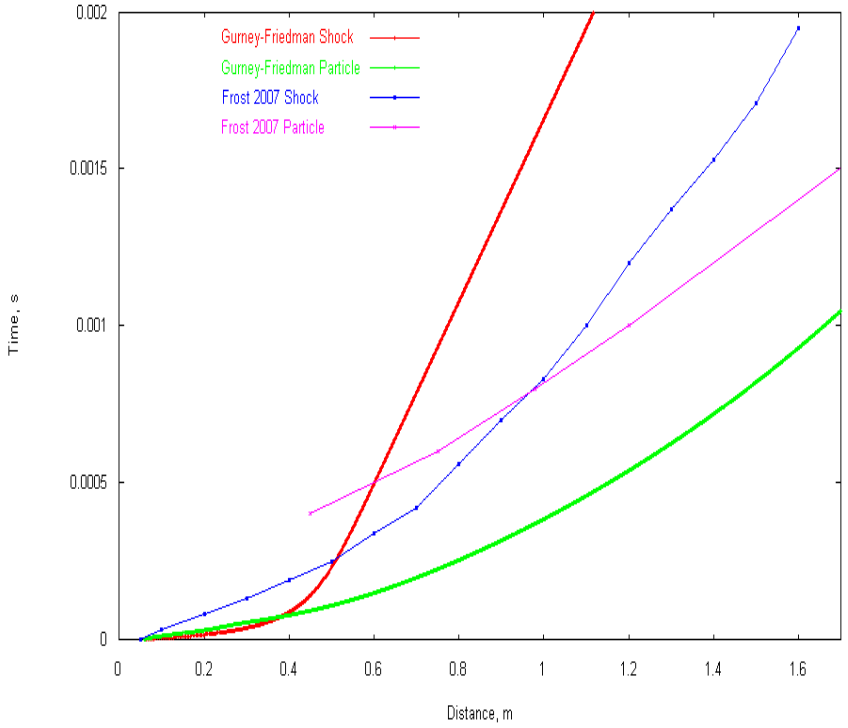

Summary/Conclusions/Recommendations

- Provides theoretical tool for study
- Important in development of heterogeneous high explosives
- Recommend model as thermally perfect gas, variable specific heats
- Improvements on secondary shock in Friedman model